



1 **Plant responses to volcanically-elevated CO₂ in two Costa Rican**
2 **forests**

3 Robert R. Bogue^{1,2}, Florian M. Schwandner^{1,3}, Joshua B. Fisher¹, Ryan Pavlick¹, Troy S. Magney¹,
4 Caroline A. Famiglietti¹, Kerry Cawse-Nicholson¹, Vineet Yadav¹, Justin P. Linick¹, Gretchen B.
5 North⁴, Eliecer Duarte⁵

6 ¹Jet Propulsion Laboratory, 4800 Oak Grove Drive, Pasadena, CA 91109, USA

7 ²Geology Department, Occidental College, 1600 Campus Road, Los Angeles, CA 90041, USA

8 ³Joint Institute for Regional Earth System Science and Engineering, University of California Los Angeles, Los
9 Angeles, CA 90095

10 ⁴Biology Department, Occidental College, 1600 Campus Road, Los Angeles, CA 90041, USA

11 ⁵OVSICORI-UNA, 2386-3000 Heredia, Costa Rica

12 Correspondence to: Florian.Schwandner@jpl.nasa.gov

13

14

15

16

17

18

19



20 **Abstract.** We explore the use of active volcanoes to determine the short- and long-term effects of elevated CO₂ on
21 tropical trees. Active volcanoes continuously but variably emit CO₂ through diffuse emissions on their flanks,
22 exposing the overlying ecosystems to elevated levels of atmospheric CO₂. We found tight correlations ($r^2=0.86$ and
23 $r^2=0.74$) between wood stable carbon isotopic composition and co-located volcanogenic CO₂ emissions for two
24 species, which documents the long-term photosynthetic incorporation of isotopically heavy volcanogenic carbon into
25 wood biomass. Measurements of leaf fluorescence and chlorophyll concentration suggest that volcanic CO₂ also has
26 measurable short-term functional impacts on select species of tropical trees. Our findings indicate significant potential
27 for future studies to utilize ecosystems located on active volcanoes as natural experiments to examine the ecological
28 impacts of elevated atmospheric CO₂ in the tropics and elsewhere. Results also point the way toward a possible future
29 utilization of ecosystems exposed to volcanically elevated CO₂ to detect changes in deep volcanic degassing by using
30 selected species of trees as sensors.

31 1 Introduction

32 Tropical forests represent about 40% of terrestrial Net Primary Productivity (NPP) worldwide, store 25% of biomass
33 carbon, and may contain 50% of all species on Earth, but the projected future responses of tropical plants to globally
34 rising levels of CO₂ are poorly understood (Leigh et al., 2004; Townsend et al., 2011). The largest source of uncertainty
35 comes from a lack of understanding of long-term CO₂ fertilization effects in the tropics (Cox et al., 2013). Reducing
36 this uncertainty would significantly improve Earth system models, advances in which would help better constrain
37 projections in future climate models (Cox et al., 2013; Friedlingstein et al., 2013). Ongoing debate surrounds the
38 question of how much more atmospheric CO₂ tropical ecosystems can absorb—the “CO₂ fertilization effect” (Gregory
39 et al., 2009; Kauwe et al., 2016; Keeling, 1973; Schimel et al., 2015).

40 Free Air CO₂ Enrichment (FACE) experiments have been conducted to probe this question, but none have
41 been conducted in tropical ecosystems (e.g. Ainsworth and Long, 2005; Norby et al., 2016). Some studies have used
42 CO₂-emitting natural springs to study plant responses to elevated CO₂, but these have been limited in scope due to the
43 small spatial areas around springs that experience elevated CO₂ (Paoletti et al., 2007; Saurer et al., 2003). These studies
44 have suffered from several confounding influences, including other gas species that accompany CO₂ emissions at
45 these springs, human disturbances, and difficulty with finding appropriate control locations. Additionally, none have
46 been conducted in the tropics (Pinkard et al., 2010). A series of studies in Yellowstone National Park (USA) used its
47 widespread volcanic hydrothermal CO₂ emissions for the same purpose, though it is not in the tropics (Sharma and
48 Williams, 2009; Tercek et al., 2008). Yellowstone was particularly suitable for this type of study, due to its protected
49 status as a National Park, and because the large areas of CO₂ emissions made control points more available (Sharma
50 and Williams, 2009; Tercek et al., 2008). These studies reported changes in rubisco and sugar production in leaves
51 similar to results from FACE experiments, suggesting that volcanically-influenced areas like Yellowstone have
52 untapped potential for studying the long-term effects of elevated CO₂ on plants.

53 Tropical ecosystems on the vegetated flanks of active volcanoes offer large and diverse ecosystems that could
54 make this type of study viable. Well over 200 active volcanoes are in the tropics (Global Volcanism Program, 2013)
55 and many of these volcanoes are heavily forested. However, fewer of these tropical volcanic forests have sufficient



56 legal protection to be a source of long-term information, and the effects of diffuse volcanic flank gas emissions on the
57 overlying ecosystems remain largely unknown. Most previous studies focused on extreme conditions, such as tree kill
58 areas associated with extraordinarily high CO₂ emissions at Mammoth Mountain, CA (USA) (Biondi and Fessenden,
59 1999; Farrar et al., 1995; Sorey et al., 1998). However, the non-lethal effects of volcanic CO₂—away from the peak
60 emission zones, but still in the theorized fertilization window—have received little attention, and could offer a new
61 approach to studying the effects of elevated CO₂ on ecosystems (Cawse-Nicholson et al., 2018). The broad flanks of
62 active volcanoes experience diffuse emissions of excess CO₂ because the underlying active magma bodies
63 continuously release gas, dominated by CO₂ transported to the surface along fault lines (Chiodini et al., 1998; Dietrich
64 et al., 2016; Farrar et al., 1995). This process has frequently been studied to understand the dynamics of active magma
65 chambers and to assess potential volcanic hazards (Chiodini et al., 1998; Sorey et al., 1998). These emissions are
66 released through faults and fractures on the flanks of the volcano (Burton et al., 2013; Pérez et al., 2011; Williams-
67 Jones et al., 2000)(see Supplementary Figure S1). Volcanic flanks through which these gases emanate are broad,
68 covering typically 50-200 km², often supporting well-developed, healthy ecosystems. Some of these faults tap into
69 shallow acid hydrothermal aquifers, but by the time these gases reach the surface of most forested volcanoes, soluble
70 and reactive volcanic gas species (e.g., SO₂, HF, HCl, H₂S) have been scrubbed out in the deep subsurface, leading to
71 a diffusely emanated gas mix of predominantly CO₂ with minor amounts of hydrogen, helium, and water vapor
72 reaching the surface (Symonds et al., 2001).

73 Trees in these locations are continuously exposed to somewhat variably elevated levels of CO₂ (eCO₂), it was
74 unclear if the trees utilize this excess CO₂. Volcanic CO₂ has a heavy δ¹³C signature typically ranging from -7 to -1
75 ‰, which is distinct from typical vegetation and noticeably heavier than typical atmospheric values (Mason et al.,
76 2017). If trees incorporate volcanic CO₂, then the stable carbon isotopic composition of wood may document the long-
77 term, possibly variable influence of volcanic CO₂ during the tree's growth. With this tracer available, volcanic
78 ecosystems could become a valuable natural laboratory to study the long-term effects of elevated CO₂ on ecosystems,
79 especially in understudied regions like the tropics. Additionally, short-term effects of eCO₂ might be revealed by plant
80 functional measurements at the leaf scale, where the additional CO₂ could increase carbon uptake in photosynthesis.

81 Here we provide preliminary results on the short- and long-term non-lethal impacts of diffuse volcanic CO₂
82 emissions on three species of tropical trees on the flanks of two active volcanoes in Costa Rica. We also explore the
83 viability of studying volcanically-influenced ecosystems to better understand potential future responses to elevated
84 CO₂, and suggest adjustments to our approach that will benefit future, similarly-motivated studies.

85 **2 Methods**

86 **2.1 Investigated locations and sampling strategy**

87 Irazú and Turrialba are two active volcanoes located ~25 and 35 km east of San José, Costa Rica. These two volcanoes
88 are divided by a large erosional basin. The two volcanoes cover approximately 315 km², which is significantly larger
89 than the average forested active volcanic edifice in Costa Rica at 122 km². The vast majority of the northern flanks of
90 Irazú and Turrialba are covered in legally protected dense old-growth forest, while the southern flanks are dominated



91 by pasture land and agriculture. Turrialba rises 3,300 m above its base and has been active for at least 75,000 years
92 with mostly fumarolic activity since its last major eruption in 1866 (Alvarado et al., 2006). It has experienced renewed
93 activity beginning in 2010, and its current activity is primarily characterized by a near-constant volcanic degassing
94 plume, episodic minor ash emissions, and fumarolic discharges at two of the summit craters, as well as significant
95 diffuse and fumarolic gas emissions across its flanks, focused along fault systems (Martini et al., 2010). Turrialba's
96 CO₂ emissions in areas proximal to the crater were calculated at 113 ± 46 tons/d (Epiard et al., 2017). The Falla Ariete,
97 a major regional fault, runs northeast-southwest through the southern part of Turrialba's central edifice and is one of
98 the largest areas of diffuse CO₂ emissions on Turrialba (Epiard et al., 2017; Rizzo et al., 2016). Atmospheric CO₂ has
99 an average $\delta^{13}\text{C}$ value of -9.2 ‰ at Turrialba, and the volcanic CO₂ released at the Ariete Fault has significantly
100 heavier $\delta^{13}\text{C}$ values clustered around -3.4 ‰ (Malowany et al., 2017).

101 Irazú has been active for at least 3,000 years, and had minor phreato-magmatic eruptions in 1963 and a single
102 hydrothermal eruption in 1994. Currently, Irazú's activity primarily consists of shallow seismic swarms, fumarolic
103 crater gas emissions, small volcanic landslides, and minor gas emissions on its northern forested flank (Alvarado et
104 al., 2006; Barquero et al., 1995). Diffuse flank emissions represent the vast majority of gas discharge from Irazú, as
105 the main crater releases 3.8 t d^{-1} of CO₂ and a small area on the north flank alone releases 15 t d^{-1} (Epiard et al., 2017).
106 Between the two volcanoes, a major erosional depression is partially occupied by extensive dairy farms, and is
107 somewhat less forested.

108 In this study, we focused on accessible areas between 2,000 and 3,300 m on both volcanoes (Fig. 1). On
109 Irazú, we sampled trees and CO₂ fluxes from the summit area to the north, near the approximately north-south striking
110 Rio Sucio fault, crossing into the area dominated by dairy farms on Irazú's lower NE slope. Our sampling locations
111 on Irazú were located along a road from the summit northward down into this low-lying area. On Turrialba, we focused
112 on an area of known strong emissions but intact forests on the SW slope, uphill of the same erosional depression, but
113 cross-cut by the major NE-SW trending active fracture system of the Falla Ariete. We sampled three main areas of
114 the Falla Ariete, each approximately perpendicularly transecting the degassing fault along equal altitude; the upper
115 Ariete fault, the lower Ariete fault, and a small basin directly east of the old Cerro Armado cinder cone on Turrialba's
116 south-western flank. We took samples at irregular intervals depending on the continued availability and specimen
117 maturity of three species present throughout the transect.

118 All transects are in areas experiencing measurable CO₂ enhancements from the Falla Ariete, but not high
119 enough to be in areas generally downwind of the prevailing crater emissions plume (Epiard et al., 2017). We avoided
120 areas that experience ash fall, high volcanic SO₂ concentrations, local anthropogenic CO₂ from farms, or that were
121 likely to have heavily acidified soil. Excessively high soil CO₂ concentrations can acidify soil, leading to negative
122 impacts on ecosystems growing there (McGee and Gerlach, 1998). Because such effects reflect by-products of extreme
123 soil CO₂ concentrations rather than direct consequences of elevated CO₂ on plants, we avoided areas with CO₂ fluxes
124 high enough to possibly cause noticeable CO₂-induced soil acidification. Light ash fall on some days likely derived
125 from atmospheric drift, as we were not sampling in areas downwind of the crater. The ash fall did not in any noticeably
126 way affect our samples, as trees showing ash accumulation on their leaves or previous damage were the exception and



127 avoided. Altitude, amount of sunlight during measurements, and aspect had no consistent correlations with any of the
128 parameters we measured.

129 2.2 Species studied

130 Our study focused on three tree species found commonly on Turrialba and Irazú: *Buddleja nitida*, *Alnus acuminata*,
131 and *Oreopanax xalapensis*. *Buddleja nitida* is a small tree with a typical stem diameter (DBH) ranging from 5 to 40
132 cm that grows at elevations of 2,000-4,000 m throughout most of Central America (Kappelle et al., 1996; Norman,
133 2000). The DBH of the individuals we measured ranged from 11.5 to 51.3 cm, with an average of 29.85 cm. It averages
134 4-15 m in height and grows primarily in early and late secondary forests (Kappelle et al., 1996; Norman, 2000). *Alnus*.
135 *acuminata* is a nitrogen-fixing pioneer species exotic to the tropics that can survive at elevations from 1,500-3,400 m,
136 although it is most commonly found between 2,000-2,800 m (Weng et al., 2004). The trees we measured had DBH
137 ranging from 14.3 to 112 cm, with an average of 57.14 cm. *Oreopanax xalapensis* thrives in early and late successional
138 forests, although it can survive in primary forests as well (Kappelle et al., 1996; Quintana-Ascencio et al., 2004). It
139 had the smallest average DBH of the three species, ranging from 6.6 to 40.9 cm, with an average of 22.71 cm.

140 2.3 CO₂ concentrations and soil diffuse flux measurements

141 We used a custom-built soil flux chamber system which contained a LI-COR 840A non-dispersive infrared CO₂ sensor
142 (LI-COR Inc., Lincoln NE, USA) to measure soil CO₂ flux. A custom-built cylindrical accumulation chamber of
143 defined volume was sealed to the ground and remained connected to the LI-COR sensor. The air within the
144 accumulation chamber was continuously recirculated through the sensor, passing through a particle filter. The sensor
145 was calibrated before deployment and performed within specifications. We recorded cell pressure and temperature,
146 ambient pressure, air temperature, GPS location, time stamps, location description, soil type and cover, wind speed
147 and direction, relative humidity, and slope, aspect, and altitude as ancillary data. In typical operation, each
148 measurement site for flux measurements was validated for leaks (visible in the live data stream display as spikes and
149 breaks in the CO₂ concentration slope), and potential external disturbances were avoided (such as vehicle traffic,
150 generators, or breathing animals and humans). Measurements were recorded in triplicate for at least 2 minutes per site.
151 Data reduction was performed using recorded time stamps in the dataset, with conservative time margins to account
152 for sensor response dead time, validated against consistent slope sections of increasing chamber CO₂. Fluxes were
153 computed using ancillary pressure and temperature measurements and the geometric chamber constant (chamber
154 volume at inserted depth, tubing volume, and sensor volume). Care was taken to not disturb the soil and overlying
155 litter inside and adjacent to, the chamber.

156 2.4 Leaf function measurements

157 Chlorophyll fluorescence measurements were conducted on leaves of all three species during the field campaign to
158 obtain information on instantaneous plant stress using an OS30p+ fluorometer (Opti-Sciences Inc., Hudson, NH,
159 USA). Five mature leaves from each individual tree were dark adapted for at least 20 minutes to ensure complete
160 relaxation of the photosystems. After dark adaptation, initial minimal fluorescence was recorded (F_0) under conditions



161 where we assume that photosystem II (PSII) was fully reduced. Immediately following the F_0 measurement, a 6,000
162 $\mu\text{mol m}^{-2} \text{s}^{-1}$ saturation pulse was delivered from an array of red LEDs at 660 nm to record maximal fluorescence
163 emission (F_m), when the reaction centers are assumed to be fully closed. From this, the variable fluorescence was
164 determined as $F_v/F_m = (F_m - F_0)/F_m$. F_v/F_m is a widely used chlorophyll fluorescence variable used to assess the
165 efficiency of PSII and, indirectly, plant stress (Baker and Oxborough, 2004). The five F_v/F_m measurements were
166 averaged to provide a representative value for each individual tree. Some trees had less than five measurements due
167 to the dark adaptation clips slipping off the leaf before measurements could be taken. Ten trees had four measurements,
168 and another six had three measurements

169 Chlorophyll concentration index (CCI) was measured with a MC-100 Apogee Instruments chlorophyll
170 concentration meter (Apogee Instruments, Inc., Logan, UT, USA). CCI was converted to chlorophyll concentration
171 ($\mu\text{mol m}^{-2}$) with the generic formula derived by Parry et al., 2014. Depending on availability, between three and six
172 leaves were measured for CCI for each tree, and then averaged to provide a single value for each tree. If leaves were
173 not within reach, a branch was pulled down or individual leaves were shot down with a slingshot and collected.
174 Photosynthetically active radiation was measured at each tree with a handheld quantum meter (Apogee Instruments,
175 Logan, UT, USA) (Table S2). Stomatal conductance to water vapor, g_s ($\text{mmol m}^{-2} \text{s}^{-1}$) was measured between 10:00-
176 14:00 hours using a steady-state porometer (SC-1, Decagon Devices, Inc., Pullman, WA, USA), calibrated before use
177 and read in manual mode. This leaf porometer was rated for humidity <90%, and humidity was sometimes above this
178 limit during our field work. Consequently, we have fewer stomatal conductance measurements than our other data
179 types.

180 **2.5 Isotopic analysis**

181 We collected wood cores from 31 individual trees at a 1.5 m height using a 5.15 mm diameter increment borer (JIM
182 GEM, Forestry Suppliers Inc., Jackson, MS, USA). Since no definable tree rings were apparent, we created a fine
183 powder for isotope analysis by drilling holes into dried cores using a dry ceramic drill bit (Dremel) along the outermost
184 5 cm of wood below the bark. The fine powder (200 mesh, 0.2 – 5 mg) was then mixed and a random sample was
185 used to extract $^{13}\text{C}/^{12}\text{C}$ ratios (to obtain $\delta^{13}\text{C}$ values against the VPDB standard), which we estimated to be
186 representative of roughly the last 2-3 years. Since we only sample the most recent years, no isotopic discrimination
187 against atmospheric ^{13}C due to preferential diffusion and carboxylation of ^{12}C , was conducted. Rather, we assume that
188 $\delta^{13}\text{C}$ values are representative of the relative amount of volcanic CO_2 vs. atmospheric CO_2 sequestered by the tree
189 over the period of growth represented in the sample. $\delta^{13}\text{C}$ values were determined by continuous flow dual isotope
190 analysis using a CHNOS Elemental Analyzer and IsoPrime 100 mass spectrometer at the University of California
191 Berkeley Center for Stable Isotope Biogeochemistry. External precision for C isotope determinations is ± 0.10 ‰. Ten
192 $\delta^{13}\text{C}$ measurements did not have corresponding soil CO_2 flux measurements due to the flux measurements being
193 unavailable for the final two days of sampling, and another 5 samples were from trees that showed signs of extreme
194 stress, such as browning leaves or anomalously low fluorescence measurements. Since the purpose of our study was
195 to explore the non-lethal effects of volcanic CO_2 on trees, during analysis we excluded all trees that were observed in



196 the field to have significant stress or that were not fully mature. After these exclusions, all remaining tree cores with
197 co-located CO₂ flux measurements were from Turrialba.

198

199 **2.6 Sulfur dioxide probability from satellite data**

200 To assess the likelihood of trees having been significantly stressed in the past by volcanic sulfur dioxide (SO₂) from
201 the central crater vents, we derived the likelihood of exposure per unit area using satellite data sensitive to SO₂ (Fig.
202 2). The Advanced Spaceborne Thermal Emission and Reflection Radiometer (ASTER), launched in December 1999
203 on NASA's Terra satellite, has bands sensitive to SO₂ emission in the thermal infrared (TIR), at ~60 m x 60 m spatial
204 resolution. We initially used ASTER Surface Radiance TIR data (AST_09T), using all ASTER observations of the
205 target area over the entirety of the ASTER mission (October 2000 until writing in late 2017). The TIR bands were
206 corrected for downwelling sky irradiance and converted into units of W m⁻² μm⁻¹. For each observation, an absorption
207 product is calculated by subtracting SO₂-insensitive from SO₂-sensitive bands:

$$208 \quad S^t = (b_{10} + b_{12}) - 2 \cdot b_{11} \quad (1)$$

209 Where S is the SO₂ index, t is an index representing the time of acquisition, b_{10} is the radiance at band 10 (8.125 -
210 8.475 μm), b_{11} is the radiance at band 11 (8.475 - 8.825 μm), and b_{12} is the radiance at band 12 (8.925 - 9.275 μm).
211 This is similar to the method of Campion et al., 2010. The granules were then separated into day and night scenes,
212 projected onto a common grid, and then thresholded to $S > 0.1$ W m⁻² μm⁻¹, and converted into a probability. The
213 output is a spatial dataset that describes the probability of an ASTER observation showing an absorption feature above
214 a 0.1 W m⁻² μm⁻¹ threshold across the entirety of the ASTER observations for day or night separately. The number of
215 scenes varies per target, but they tend to be between 200-800 observations in total, over the 17 year time period of
216 satellite observations. However, certain permanent features, such as salt pans, show absorption features in band 11
217 and therefore have high ratios for the algorithm used. We therefore used a second method that seeks to map transient
218 absorption features. For this method, we subtract the median from each S^t , yielding a median deviation stack. By
219 plotting the maximum deviations across all observations, we then get a map of transient absorption features, in our
220 case this is mostly volcanic SO₂ plumes, which map out the cumulative position of different plume observations well.
221 To speed up processing, some of the retrieval runs were binned in order to increase the signal-to-noise ratio, since the
222 band difference can be rather noisy.

223 **2.7 Modelling the anthropogenic CO₂ influence from inventory data**

224 We assessed the likelihood of anthropogenic CO₂, enhancements of air from San Jose, Costa Rica's capital and main
225 industrial and population center, influencing our measurements. We used a widely applied Flexible Particle Dispersion
226 Model (Eckhardt et al., 2017; Stohl et al., 1998, 2005; Stohl and Thomson, 1999) in a forward mode (Stohl et al.,
227 2005) to simulate the downwind concentrations of CO₂ in the atmosphere (e.g. Belikov et al., 2016), due to inventory-
228 derived fossil fuel (FF) emissions in our study area for the year 2015 (Fig. 2). The National Centers for Environmental
229 Prediction (NCEP) - Climate Forecast System Reanalysis (CFSR) 2.5° horizontal resolution meteorology (Saha et al.,
230 2010b, 2010a), and 1-km Open-Source Data Inventory for Anthropogenic CO₂ (ODIAC; Oda and Maksyutov, 2011)



231 emissions for 2015 were used to drive the Flexpart model. The CO₂ concentrations were generated at a 1 km spatial
232 resolution within three levels of the atmosphere (0-100, 100-300, 300-500 meters) that are possibly relevant to forest
233 canopies in Costa Rica. However, to assess the magnitude of enhancements we only used CO₂ concentrations observed
234 within the lowest level of the atmosphere. Validation of the model with direct observations was not required because
235 we were only interested in ensuring that anthropogenic CO₂ dispersed upslope from San José was not having a
236 significant effect on our study area. The actual concentration of CO₂ and any biogenic influence in the modelled area
237 was irrelevant because the spatial distribution of anthropogenic CO₂ was the only factor relevant for this test. 2015
238 was used as a representative year for simulating the seasonal cycle of CO₂ concentrations that would be present in any
239 particular year.

240 **3 Results**

241 **3.1 Volcanic CO₂ emissions through the soil**

242 We measured CO₂ flux emitted through the soil at 66 points over four days (Fig. 1). The first eight points were on
243 Irazú, and the rest were located near the Ariete Fault on Turrialba. Mean soil CO₂ flux values over the entire sampling
244 area varied from 3 to 37 g m⁻² day⁻¹, with an average of 11.6 g m⁻² day⁻¹ and a standard deviation of 6.6 g m⁻² day⁻¹. A
245 12-bin histogram of mean CO₂ flux shows a bimodal right-skewed distribution with a few distinct outliers (Fig. 3).
246 Fluxes were generally larger on Irazú than on Turrialba. This result agrees with previous studies which showed that
247 the north flank of Irazú has areas of extremely high degassing, whereas most of our sampling locations on Turrialba
248 were in areas that had comparatively lower diffuse emissions (Epiard et al., 2017; Stine and Banks, 1991). We used a
249 cumulative probability plot to identify different populations of CO₂ fluxes (Fig. 3) (Cardellini et al., 2003; Sinclair,
250 1974). Our measurements and literature data confirm that ecosystems growing in these locations are consistently
251 exposed to excess volcanic CO₂, which may impact chlorophyll fluorescence, chlorophyll concentrations, and stomatal
252 conductance of nearby trees.

253 We created an inventory-based model of anthropogenic CO₂ emissions from the San José urban area, parts
254 of which are less than 15 km from some of our sampling locations (Fig. 2). Our model shows that CO₂ emitted from
255 San José is blown west to south-west by prevailing winds. Our study area is directly east of San José, and as such is
256 unaffected by anthropogenic CO₂ from San Jose, which is the only major urban area near Turrialba and Irazú.
257 Additionally, we used ASTER data to map probabilities of SO₂ across Costa Rica, as a possible confounding factor.
258 The active craters of both Turrialba and Irazú emit measurable amounts of SO₂, which is reflected by the high SO₂
259 probabilities derived there (Fig. 2). Our study area is on the flanks of the volcano, where SO₂ probability is minimal.
260 Most other volcanoes in Costa Rica emit little to no SO₂ on a decadal time scale, shown by the low or non-existent
261 long-term SO₂ probabilities over the other volcanoes in Costa Rica (white polygons in Fig. 2).

262 **3.2 Tree core isotopes**

263 Bulk wood δ¹³C measurements ranged from -24.03 to -28.12 ‰, with most being clustered around -26 ‰ (Fig. 4). A
264 5-bin histogram of all δ¹³C measurements shows a slightly right-skewed unimodal normal distribution, with an average



265 of -26.37 ‰ and a standard deviation of 0.85 ‰. *A. acuminata* and *O. xalapensis* have nearly identical averages (-
266 26.14 and -25.97 ‰, respectively), while *B. nitida* has a noticeably lighter average of -27.02 ‰. As CO₂ flux increased,
267 the wood cores contained progressively higher amounts of ¹³C for two of the three species. Tree core δ¹³C showed no
268 relationship with stomatal conductance for any species.

269 3.3 Plant function (Fluorescence, Chlorophyll, Stomatal Conductance)

270 After excluding visibly damaged trees, leaf fluorescence, expressed as Fv/Fm, was very high in most samples. Fv/Fm
271 ranged from 0.75 to 0.89, with most measurements clustering between 0.8 and 0.85 (Fig. 5). The fluorescence data
272 has a left-skewed unimodal distribution. The leaf fluorescence (Fv/Fm) values for *A. acuminata* had a strong positive
273 correlation with soil CO₂ flux ($r^2=0.69$, $p<.05$), while the other two species showed no correlation. No confounding
274 factors measured were correlated with Fv/Fm for any species. In general, *B. nitida* had the highest Fv/Fm values, and
275 *A. acuminata* and *O. xalapensis* had similar values except for a few *O. xalapensis* outliers. Chlorophyll concentration
276 measurements were highly variable, ranging from 260 to 922 μmol m⁻², with an average of 558 μmol m⁻² and a standard
277 deviation of 162 μmol m⁻² (Fig. 6). Chlorophyll concentration had a complicated right-skewed bimodal distribution,
278 likely due to the noticeably different averages for each species. *A. acuminata* and *O. xalapensis* both displayed weak
279 correlations between chlorophyll concentration and soil CO₂ flux ($r^2=0.38$ and $r^2=0.28$, respectively), but their
280 trendlines were found to be almost perpendicular (Fig. 6). As CO₂ flux increased, *A. acuminata* showed a slight
281 increase in chlorophyll concentration, while *O. xalapensis* had significant decreases in chlorophyll concentration. *B.*
282 *nitida* individuals growing on steeper slopes had significantly lower chlorophyll concentration measurements ($r^2=0.42$,
283 $p<.05$) than those on gentler slopes, a trend not expressed by either of the other two species ($r^2=0.01$ for both),
284 demonstrating no significant influence of slope across the majority of samples. Stomatal conductance ranged from
285 83.5 to 361 mmol H₂O m⁻² s⁻¹, with an average of 214 mmol H₂O m⁻² s⁻¹ and a standard deviation of 73.5 mmol H₂O
286 m⁻² s⁻¹. Distribution was bimodal, with peaks around 150 and 350 mmol H₂O m⁻² s⁻¹. *A. acuminata* had a moderate
287 positive correlation ($r^2=0.51$) with soil CO₂ flux, but it was not statistically significant due to a lack of data points
288 (Fig. 7) – however this is a result consistent with the observed higher chlorophyll concentration (Fig. 6). The other
289 two species displayed no correlation with soil CO₂ flux. *B. nitida* had a moderate negative correlation ($r^2=0.61$) with
290 slope, similar to its correlation between chlorophyll concentration and slope.

291 4 Discussion

292 4.1 Long-term plant uptake of volcanic CO₂

293 Turrialba and Irazú continuously emit CO₂ through their vegetated flanks, but prior to this study it was unknown if
294 the trees growing there were utilizing this additional isotopically heavy volcanic CO₂. All tree cores with
295 corresponding CO₂ flux measurements were from areas proximal to the Ariete Fault on Turrialba, where atmospheric
296 and volcanic δ¹³C have significantly different values (-9.2 and -3.4 ‰, respectively) (Malowany et al., 2017). If the
297 trees assimilate volcanic CO₂ through their stomata, then we would expect wood δ¹³C to trend towards heavier values
298 as diffuse volcanic CO₂ flux increases. After excluding damaged samples and stressed trees, δ¹³C was strongly



299 correlated with soil CO₂ flux for both *B. nitida* and *O. xalapensis* (Fig. 4). *A. acuminata* did not have a statistically
300 significant correlation between soil CO₂ flux and δ¹³C, likely because it had the fewest data points and a minimal
301 range of CO₂ and δ¹³C values. The strong positive correlations between CO₂ flux and increasingly heavy δ¹³C values
302 suggest that the trees have consistently photosynthesized with isotopically heavy excess volcanic CO₂ over the last
303 few years and are therefore growing in eCO₂ conditions. Assuming that all variations in δ¹³C are caused by the
304 incorporation of heavy volcanic CO₂, we can calculate the average concentration of the mean volcanic excess CO₂ in
305 the air the plants are exposed to, with a mass balance equation (Eq. 2):

$$306 \quad C_v = \frac{C_b(\delta_b - \delta_m)}{(\delta_m - \delta_v)} \quad (2)$$

307 where C_v is the mean volcanic excess component of the CO₂ concentration in air, C_b is the atmospheric “background”
308 (i.e., non-volcanic) CO₂ concentration, δ_b is atmospheric δ¹³C, δ_m is the difference between background wood δ¹³C
309 and another wood δ¹³C measurement subtracted from atmospheric δ¹³C, and δ_v is δ¹³C of the volcanic CO₂.
310 Background wood δ¹³C is the value of the point for each species with the lowest CO₂ flux (Fig. 4), and the other wood
311 δ¹³C measurement is any other point from the same species. Values for δ_v and δ_b are taken from Malowany et al. 2017,
312 and C_b is assumed to be 400 ppm. For the tree core with the highest measured CO₂ flux for *O. xalapensis*, this equation
313 yields a mean excess volcanic CO₂ concentration of 155 ppm, bringing the combined mean atmospheric (including
314 volcanic) CO₂ concentration these trees are exposed to, to ~555 ppm. For *B. nitida* this equation yields 190 ppm of
315 mean excess volcanic CO₂ at the highest flux location, for a combined total mean of ~590 ppm CO₂. These calculations
316 show that trees in our study area have been consistently exposed to significantly elevated concentrations of CO₂,
317 reflective of predicted atmospheric conditions 60-80 years into the future, assuming a 2 ppm y⁻¹ mean atmospheric
318 growth rate (Peters et al., 2007), Additional measurements of tree core δ¹³C and associated soil CO₂ fluxes would help
319 corroborate our observations, which were based on a limited number of data points. Tree ring ¹⁴C content in
320 volcanically active areas has been linked to variations in volcanic CO₂ emissions, and comparing patterns of δ¹³C to
321 ¹⁴C measurements for the same wood samples could provide additional confirmation of this finding (Evans et al.,
322 2010; Lefevre et al., 2017; Lewicki et al., 2014).

323 Our data demonstrate that CO₂ fluxes through the soil are a representative relative measure for eCO₂
324 exposure of overlying tree canopies. Forest canopy exposure to volcanic CO₂ will vary over time, as will volcanic
325 eCO₂, once emitted through the soil into the sub-canopy atmosphere, the gas experiences highly variable thermal and
326 wind disturbances which significantly affect dispersion of CO₂ on minute to minute, diurnal, and seasonal timescales
327 (Staebler and Fitzjarrald, 2004; Thomas, 2011). These processes cause in-canopy measurements of CO₂ concentration
328 to be highly variable, making instantaneous concentration measurements in a single field campaign not representative
329 of long-term relative magnitudes of CO₂ exposure. Soil CO₂ fluxes are less tied to atmospheric conditions, and are
330 primarily externally modulated by rainfall which increases soil moisture and therefore lowers the soil’s gas
331 permeability (Camarda et al., 2006; Viveiros et al., 2009). These fluxes can also be affected by variations in barometric
332 pressure, but both of these factors are easily measurable and therefore can be factored in when conducting field work
333 (Viveiros et al., 2009). Assuming the avoidance of significant rainfall and pressure spikes during sampling
334 (measurements were conducted in the dry season and no heavy rains or significant meteorological variations in
335 pressure occurred during field work), measuring the input of CO₂ into the sub-canopy atmosphere as soil CO₂ fluxes



336 is therefore expected to better represent long-term input and exposure of tree canopies to eCO₂ than direct
337 instantaneous measurements of sub-canopy CO₂ concentration. Previous studies at Turrialba have shown that local
338 volcanic CO₂ flux is relatively constant on monthly to yearly timescales (de Moor et al., 2016). Therefore, current soil
339 CO₂ fluxes should give relatively accurate estimates of CO₂ exposure over time. This paper corroborates that
340 expectation by demonstrating strong correlations between volcanically enhanced soil CO₂ emissions with stable
341 carbon isotope signals of these emissions documented in the trees' xylem.

342 A study at the previously mentioned Mammoth Mountain tree kill area examined the connection between
343 δ¹³C and volcanic CO₂ fluxes, but focused on the difference between trees killed by extreme CO₂ conditions and those
344 that were still alive (Biondi and Fessenden, 1999). They concluded that the changes in δ¹³C that they observed were
345 due to extreme concentrations of CO₂ (soil CO₂ concentrations of up to 100%) impairing the functioning of root
346 systems, leading to closure of stomata and water stress (Biondi and Fessenden, 1999). CO₂ does not inherently harm
347 trees, but the extreme CO₂ concentrations (up to 100% soil CO₂) at the Mammoth Mountain area caused major soil
348 acidification, which led to the tree kill (McGee and Gerlach, 1998). We have evidence that those processes are not
349 affecting our δ¹³C measurements, and that variations in our δ¹³C measurements are more likely to be caused by direct
350 photosynthetic incorporation of heavy volcanic CO₂. Our δ¹³C measurements have no statistically significant
351 correlation with stomatal conductance, which suggests that our heavier δ¹³C measurements are not linked to stomatal
352 closure. Additionally, none of the trees displayed obvious signs of stress, from water or other factors, as indicated by
353 their high fluorescence and chlorophyll concentration values and lack of visible indicators of stress; specifically, our
354 values of Fv/Fm ~0.8 indicate that PSII was operating efficiently in most of the trees we measured (Baker and
355 Oxborough, 2004). The Mammoth Mountain tree kill areas have several orders of magnitude higher CO₂ fluxes (well
356 over 10,000 g m⁻² day⁻¹) than the areas we sampled (up to 38 g m⁻² day⁻¹), making it much more likely that stress from
357 soil acidification would be causing stomatal closure and affecting wood δ¹³C measurements at Mammoth Mountain
358 (Biondi and Fessenden, 1999; McGee and Gerlach, 1998; Werner et al., 2014). In contrast, most of the diffuse
359 degassing at Turrialba does not lead to soil acidification or pore space saturation, as is evident in our own and others'
360 field data (e.g., Epiard et al 2017). Thus, changes in our δ¹³C values are best explained by direct photosynthetic
361 incorporation of isotopically heavy volcanic CO₂. To the best of our knowledge, this is the first time that a direct
362 correlation between volcanic soil CO₂ flux and wood δ¹³C has been documented. Future studies should explore this
363 correlation further, as our findings are based on a limited sample size.

364 4.2 Short-term species response to eCO₂

365 Short-term plant functional responses at the leaf level to elevated CO₂ were highly species-dependent. *B. nitida* had
366 no statistically significant functional responses to soil CO₂ flux and *O. xalapensis* only had a weak negative correlation
367 between soil CO₂ flux and chlorophyll concentration (Fig. 6). *A. acuminata*, a nitrogen fixing species, was the only
368 species with a consistent and positive functional response to elevated CO₂, displaying a strong positive correlation
369 with fluorescence and a weak positive correlation with chlorophyll concentration and stomatal conductance (Figs. 5-
370 7). The lack of response in *B. nitida* and *O. xalapensis* could be due to nitrogen limitation, a factor that would not
371 affect *A. acuminata* due to its nitrogen fixing capability. Previous studies have found that nitrogen availability strongly



372 controls plant responses to eCO₂ in a variety of ecosystems, including grasslands and temperate forests (Garten et al.,
373 2011; Hebeisen et al., 1997; Lüscher et al., 2000; Norby et al., 2010). Nitrogen limitation has been posited to be an
374 important factor in tropical montane cloud forests, and may be contributing to the lack of responses in *B. nitida* and
375 *O. xalapensis* (Tanner et al., 1998). Due to the exploratory nature of our study, we do not have a large enough dataset
376 to conclude that the nitrogen fixing capability of species like *A. acuminata* is the cause for its positive response to
377 volcanically elevated CO₂, as has been speculated before (Schwandner et al., 2004), but it is a possible correlation that
378 deserves further investigation. Future studies should explore this correlation further to determine the extent of nitrogen
379 limitation at Turrialba and Irazú and its impacts on plant responses to eCO₂.

380 4.3 Trees as volcanic CO₂ sensors

381 Beyond the potential to advance our understanding of tropical forest ecosystem responses to elevated CO₂, our results
382 have importance to the volcanological community. If the link between δ¹³C and volcanic CO₂ is as strong as our results
383 suggest, it could be used to establish temporal histories of volcanic CO₂ emissions at previously unmonitored
384 volcanoes, and fill observational gaps in volcanic activity histories. The data presented in this paper represent
385 approximately the past 2-3 years of growth, but taking δ¹³C measurements at regular intervals on the remainder of a
386 tree core should provide a history of temporal variations in volcanic CO₂ emissions. This has significant volcanological
387 applications, as it would provide a powerful new tool to study volcanic CO₂ emissions in a temporal context.
388 Variations in tree ring ¹⁴C content have been shown to correlate well with variations in volcanic CO₂ flux, but ¹⁴C is
389 relatively expensive and a limited number of labs are capable of making these measurements (Evans et al., 2010;
390 Lefevre et al., 2017; Lewicki and Hilley, 2014). δ¹³C measurements are more accessible, allowing for substantially
391 more data to be acquired compared to ¹⁴C. Comparing wood δ¹³C records of past CO₂ fluxes to historical records of
392 eruptions could help establish patterns of CO₂ fluxes at volcanoes that have minimal CO₂ flux datasets available.
393 These patterns of CO₂ flux could then be compared to current volcanic CO₂ flux data and historical eruption records
394 to fill gaps in the historical and monitoring records – a boon for volcano researchers and observatories using pattern
395 recognition to improve eruption prediction capabilities (Newhall et al., 2017; Pyle, 2017; Sparks et al., 2012).
396 Independent validation, and calibration by wood core dendrochronology via ¹⁴C, tree rings, or chemical event tracers
397 like sulfur spikes, could significantly advance the concept of using wood carbon as archives of past degassing activity.
398 Furthermore, knowledge of short-term real-time response of leaves to variations in volcanic flank CO₂, which is more
399 likely to represent deeper processes inside volcanoes than crater-area degassing (Camarda et al., 2012), may permit
400 the use of trees as sensors of transient changes in volcanic degassing indicative of volcanic reactivation and deep
401 magma movement possibly leading up to eruptions (Camarda et al., 2012; Pieri et al., 2016; Schwandner et al., 2017;
402 Shinohara et al., 2008; Werner et al., 2013).

403 4.4 Lessons Learned for Future Studies

404 This exploratory study reveals significant new potential for future studies to utilize the volcanically enhanced CO₂
405 emissions approach to study tropical ecosystem responses to eCO₂. These two Costa Rican volcanoes, as well as
406 several other volcanoes in the country, have large areas of relatively undisturbed old-growth forest on their broad



407 flanks, making them ideal study areas for examining responses of ecosystems to eCO₂. However, there are several
408 challenges future studies should take into consideration if attempting to expand upon this preliminary study. Given
409 the enormous tropical species diversity and the need to control for confounding factors, large datasets will be needed
410 to answer these questions conclusively. Unfortunately, field data can be difficult to acquire in these environments as
411 the terrain is rugged and can be challenging to work in. A remote sensing approach using airborne measurements,
412 combined with targeted representative ground campaign field work for validation, could provide sufficiently large
413 data sets to represent species diversity and conditions in conjunction with ground based measurements. Many of the
414 datatypes that would be useful for this type of study can be acquired from airborne platforms, and remote sensing
415 instruments can quickly produce the massive datasets that would be required to provide more comprehensive answers
416 to these questions (Cawse-Nicholson et al., 2018). There are six other forested volcanoes in Costa Rica which are
417 actively degassing CO₂ through their flanks (Epiard et al., 2017; Liegler, 2016; Melián et al., 2007; de Moor et al.,
418 2016; Williams-Jones, 1997; Williams-Jones et al., 2000), that would also be viable for this type of study (see polygons
419 in Fig. 2), and datasets from those volcanoes would be helpful as they would provide a wider range of altitudes,
420 precipitation levels, temperatures, and other environmental factors that would help isolate the effects of eCO₂.

421 5 Conclusions

422 We identified multiple areas of dense old-growth tropical forest on two Costa Rican active volcanoes that are
423 consistently and continuously exposed to volcanically-elevated levels of atmospheric CO₂, diffusively emitted through
424 soils into overlying forests. These isotopically heavy excess volcanic CO₂ emissions are well correlated with increases
425 in heavy carbon signatures in wood cores from two species of tropical trees, suggesting long-term incorporation of
426 enhanced levels of volcanically emitted CO₂ into biomass. Confounding factors that are known to influence δ¹³C
427 values in wood appear not to have affected our measurements, indicating that the heavier wood isotope values are
428 most likely caused by photosynthetic incorporation of volcanic excess CO₂. One of the three species studied (*A.*
429 *acuminata*) has consistent positive correlations between instantaneous plant function measurements and diffuse CO₂
430 flux measurements, indicating that short-term variations in elevated CO₂ emissions may measurably affect trees
431 growing in areas of diffuse volcanic emissions. These observations reveal significant potential for future studies to
432 use these areas of naturally elevated CO₂ to study ecosystem responses to elevated CO₂, and to use trees as sensors of
433 changing degassing behavior of volcanic flanks, indicative of deep magmatic processes.

434

435 *Data availability.* Data can be found in Table S1 and Table S2 in the supplement or can be requested from Florian
436 Schwandner (Florian.Schwandner@jpl.nasa.gov).

437

438 *Author contributions.* FMS and JBF designed the study, and RRB, FMS, JBF, and ED conducted the field work and
439 collected all samples and data with some of the equipment borrowed from GN, who helped interpret the results. TSM
440 processed the samples for analysis. JPL conducted the SO₂ analysis, wrote the related methods subsection, and helped
441 interpret the results. VY modelled the anthropogenic CO₂ emissions, wrote the related methods subsection, and helped



442 interpret the results. CAF created the combined figure showing the CO₂ and SO₂ results and assisted in writing the
443 manuscript. RRB wrote the publication, with contributions from all co-authors.

444

445 *Competing interests.* The authors declare that they have no conflict of interest.

446 **Acknowledgements**

447 We are grateful for LI-COR, Inc. (Lincoln, NE, USA) providing us a loaner CO₂ sensor for field work in Costa Rica.
448 We thank Rizalina Schwandner for engineering assistance during sensor integration, OVSICORI (Observatorio
449 Vulcanológico y Sismológico de Costa Rica, the Costa Rican volcano monitoring authority) for logistical and permit
450 support, SINAC (Sistema Nacional de Áreas de Conservación, the Costa Rican National Parks Service) for access at
451 Turrialba volcano, as well as Mr. Marco Antonio Otárola Rojas (Universidad Nacional Autónoma de Costa Rica –
452 ICOMVIS) for invaluable help in the field. Incidental funding is acknowledged from the S.W. Hartman Fund at
453 Occidental College for funding R.R.B.'s field expenses, as well as the Jet Propulsion Laboratory's YIP (Year-round
454 Internship Program) and the Jet Propulsion Laboratory Education Office for funding and support for R.R.B. F.M.S.'s
455 UCLA contribution to this work was supported by Jet Propulsion Laboratory subcontract 1570200. Part of the research
456 described in this paper was carried out at the Jet Propulsion Laboratory, California Institute of Technology, under a
457 contract with the National Aeronautics and Space Administration.

458 **References**

- 459 Ainsworth, E. A. and Long, S. P.: What have we learned from 15 years of free-air CO₂ enrichment (FACE)? A meta-
460 analytic review of the responses of photosynthesis, canopy properties and plant production to rising CO₂, *New Phytol.*,
461 165(2), 351–372, doi:10.1111/j.1469-8137.2004.01224.x, 2005.
- 462 Alvarado, G. E., Carr, M. J., Turrin, B. D., Swisher, C. C., Schmincke, H.-U. and Hudnut, K. W.: Recent volcanic
463 history of Irazú volcano, Costa Rica: Alternation and mixing of two magma batches, and pervasive mixing, in *Special*
464 *Paper 412: Volcanic Hazards in Central America*, vol. 412, pp. 259–276, Geological Society of America., 2006.
- 465 Baker, N. R. and Oxborough, K.: Chlorophyll Fluorescence as a Probe of Photosynthetic Productivity, in *Chlorophyll*
466 *a Fluorescence*, pp. 65–82, Springer, Dordrecht., 2004.
- 467 Barquero, R., Lesage, P., Metaxian, J. P., Creusot, A. and Fernández, M.: La crisis sísmica en el volcán Irazú en 1991
468 (Costa Rica), *Rev. Geológica América Cent.*, 0(18), doi:10.15517/rgac.v0i18.13494, 1995.
- 469 Belikov, D. A., Maksyutov, S., Yaremchuk, A., Ganshin, A., Kaminski, T., Blessing, S., Sasakawa, M., Gomez-
470 Pelaez, A. J. and Starchenko, A.: Adjoint of the global Eulerian–Lagrangian coupled atmospheric transport model (A-
471 GELCA v1.0): development and validation, *Geosci. Model Dev.*, 9(2), 749–764, doi:10.5194/gmd-9-749-2016, 2016.
- 472 Biondi, F. and Fessenden, J. E.: Response of lodgepole pine growth to CO₂ degassing at Mammoth Mountain,
473 California, *Ecol. Brooklyn*, 80(7), 2420–2426, 1999.
- 474 Burton, M. R., Sawyer, G. M. and Granieri, D.: Deep Carbon Emissions from Volcanoes, *Rev. Mineral. Geochem.*,
475 75(1), 323–354, doi:10.2138/rmg.2013.75.11, 2013.



- 476 Camarda, M., Gurrieri, S. and Valenza, M.: CO₂ flux measurements in volcanic areas using the dynamic concentration
477 method: Influence of soil permeability, *J. Geophys. Res. Solid Earth*, 111(B5), B05202, doi:10.1029/2005JB003898,
478 2006.
- 479 Camarda, M., De Gregorio, S. and Gurrieri, S.: Magma-ascent processes during 2005–2009 at Mt Etna inferred by
480 soil CO₂ emissions in peripheral areas of the volcano, *Chem. Geol.*, 330–331, 218–227,
481 doi:10.1016/j.chemgeo.2012.08.024, 2012.
- 482 Campion, R., Salerno, G. G., Coheur, P.-F., Hurtmans, D., Clarisse, L., Kazahaya, K., Burton, M., Caltabiano, T.,
483 Clerbaux, C. and Bernard, A.: Measuring volcanic degassing of SO₂ in the lower troposphere with ASTER band ratios,
484 *J. Volcanol. Geotherm. Res.*, 194(1–3), 42–54, doi:10.1016/j.jvolgeores.2010.04.010, 2010.
- 485 Cardellini, C., Chiodini, G. and Frondini, F.: Application of stochastic simulation to CO₂ flux from soil: Mapping and
486 quantification of gas release, *J. Geophys. Res. Solid Earth*, 108(B9), 2425, doi:10.1029/2002JB002165, 2003.
- 487 Cawse-Nicholson, K., Fisher, J. B., Famiglietti, C. A., Braverman, A., Schwandner, F. M., Lewicki, J. L., Townsend,
488 P. A., Schimel, D. S., Pavlick, R., Borman, K., Ferraz, A. A., Ye, Z., Kang, L. E., Ma, P., Bogue, R., Youmans, T.
489 and Pieri, D. C.: Ecosystem responses to elevated CO₂ using airborne remote sensing at Mammoth Mountain,
490 California, *Biogeosciences Discuss.*, 2018.
- 491 Chiodini, G., Cioni, R., Guidi, M., Raco, B. and Marini, L.: Soil CO₂ flux measurements in volcanic and geothermal
492 areas, *Appl. Geochem.*, 13(5), 543–552, doi:10.1016/S0883-2927(97)00076-0, 1998.
- 493 Cox, P., Pearson, D., Booth, B., Friedlingstein, P., Huntingford, C., Jones, C. and Luke, M.: Sensitivity of tropical
494 carbon to climate change constrained by carbon dioxide variability., 2013.
- 495 Dietrich, V. J., Fiebig, J., Chiodini, G. and Schwandner, F. M.: Fluid Geochemistry of the Hydrothermal System, in
496 Nisyros Volcano, edited by V. J. Dietrich, E. Lagios, and O. Bachmann, p. 339, Springer, Berlin., 2016.
- 497 Eckhardt, S., Cassiani, M., Evangeliou, N., Sollum, E., Pisso, I. and Stohl, A.: Source–receptor matrix calculation for
498 deposited mass with the Lagrangian particle dispersion model FLEXPART v10.2 in backward mode, *Geosci. Model
499 Dev. Katlenburg-Lindau*, 10(12), 4605–4618, doi:http://dx.doi.org/10.5194/gmd-10-4605-2017, 2017.
- 500 Epiard, M., Avard, G., de Moor, J. M., Martínez Cruz, M., Barrantes Castillo, G. and Bakkar, H.: Relationship between
501 Diffuse CO₂ Degassing and Volcanic Activity. Case Study of the Poás, Irazú, and Turrialba Volcanoes, Costa Rica,
502 *Front. Earth Sci.*, 5, doi:10.3389/feart.2017.00071, 2017.
- 503 Evans, W. C., Bergfeld, D., McGeehin, J. P., King, J. C. and Heasler, H.: Tree-ring ¹⁴C links seismic swarm to CO₂
504 spike at Yellowstone, USA, *Geology*, 38(12), 1075–1078, 2010.
- 505 Farrar, C. D., Sorey, M. L., Evans, W. C., Howle, J. F., Kerr, B. D., Kennedy, B. M., King, C.-Y. and Southon, J. R.:
506 Forest-killing diffuse CO₂ emission at Mammoth Mountain as a sign of magmatic unrest, *Nature*, 376(6542), 675–
507 678, doi:10.1038/376675a0, 1995.
- 508 Friedlingstein, P., Meinshausen, M., Arora, V. K., Jones, C. D., Anav, A., Liddicoat, S. K. and Knutti, R.:
509 Uncertainties in CMIP5 Climate Projections due to Carbon Cycle Feedbacks, *J. Clim.*, 27(2), 511–526,
510 doi:10.1175/JCLI-D-12-00579.1, 2013.
- 511 Garten, C. T., Iversen, C. M. and Norby, R. J.: Litterfall ¹⁵N abundance indicates declining soil nitrogen availability
512 in a free-air CO₂ enrichment experiment, *Ecology*, 92(1), 133–139, doi:10.1890/10-0293.1, 2011.



- 513 Global Volcanism Program: Volcanoes of the World, v. 4.6.5, edited by E. Venzke, Smithsonian Inst.,
514 doi:<https://dx.doi.org/10.5479/si.GVP.VOTW4-2013>, 2013.
- 515 Gregory, J. M., Jones, C. D., Cadule, P. and Friedlingstein, P.: Quantifying Carbon Cycle Feedbacks, *J. Clim.*, 22(19),
516 5232–5250, doi:10.1175/2009JCLI2949.1, 2009.
- 517 Hebeisen, T., Lüscher, A., Zanetti, S., Fischer, B., Hartwig, U., Frehner, M., Hendrey, G., Blum, H. and Nösberger*,
518 J.: Growth response of *Trifolium repens* L. and *Lolium perenne* L. as monocultures and bi-species mixture to free air
519 CO₂ enrichment and management, *Glob. Change Biol.*, 3(2), 149–160, doi:10.1046/j.1365-2486.1997.00073.x, 1997.
- 520 Kappelle, M., Geuze, T., Leal, M. E. and Cleef, A. M.: Successional age and forest structure in a Costa Rican upper
521 montane *Quercus* forest, *J. Trop. Ecol.*, 12(05), 681–698, doi:10.1017/S0266467400009871, 1996.
- 522 Kauwe, M. G. D., Keenan, T. F., Medlyn, B. E., Prentice, I. C. and Terrer, C.: Satellite based estimates underestimate
523 the effect of CO₂ fertilization on net primary productivity, *Nat. Clim. Change*, 6(10), 892, doi:10.1038/nclimate3105,
524 2016.
- 525 Keeling, C. D.: The Carbon Dioxide Cycle: Reservoir Models to Depict the Exchange of Atmospheric Carbon Dioxide
526 with the Oceans and Land Plants, in *Chemistry of the Lower Atmosphere*, edited by S. I. Rasool, pp. 251–329, Springer
527 US, Boston, MA., 1973.
- 528 Lefevre, J.-C., Gillot, P.-Y., Cardellini, C., Gresse, M., Lesage, L., Chiodini, G. and Oberlin, C.: Use of the
529 Radiocarbon Activity Deficit in Vegetation as a Sensor of CO₂ Soil Degassing: Example from La Solfatara (Naples,
530 Southern Italy), *Radiocarbon*, 1–12, doi:10.1017/RDC.2017.76, 2017.
- 531 Leigh, E. G., Losos, E. C. and Research, N. B. of E.: Tropical forest diversity and dynamism : findings from a large-
532 scale network, Chicago, Ill.; London : The University of Chicago Press. [online] Available from:
533 <http://trove.nla.gov.au/version/12851528> (Accessed 25 September 2017), 2004.
- 534 Lewicki, J. L. and Hilley, G. E.: Multi-scale observations of the variability of magmatic CO₂ emissions, Mammoth
535 Mountain, CA, USA, *J. Volcanol. Geotherm. Res.*, 284(Supplement C), 1–15, doi:10.1016/j.jvolgeores.2014.07.011,
536 2014.
- 537 Lewicki, J. L., Hilley, G. E., Shelly, D. R., King, J. C., McGeehin, J. P., Mangan, M. and Evans, W. C.: Crustal
538 migration of CO₂-rich magmatic fluids recorded by tree-ring radiocarbon and seismicity at Mammoth Mountain, CA,
539 USA, *Earth Planet. Sci. Lett.*, 390, 52–58, doi:10.1016/j.epsl.2013.12.035, 2014.
- 540 Liegler, A.: Diffuse CO₂ degassing and the origin of volcanic gas variability from Rincon de la Vieja, Miravalles, and
541 Tenorio volcanoes, Guanacaste province, Costa Rica, Open Access Masters Thesis Mich. Technol. Univ. [online]
542 Available from: <http://digitalcommons.mtu.edu/etdr/97>, 2016.
- 543 Lüscher, A., Hartwig, U. A., Suter, D. and Nösberger, J.: Direct evidence that symbiotic N₂ fixation in fertile grassland
544 is an important trait for a strong response of plants to elevated atmospheric CO₂, *Glob. Change Biol.*, 6(6), 655–662,
545 doi:10.1046/j.1365-2486.2000.00345.x, 2000.
- 546 Malowany, K. S., Stix, J., de Moor, J. M., Chu, K., Lacrampe-Couloume, G. and Sherwood Lollar, B.: Carbon isotope
547 systematics of Turrialba volcano, Costa Rica, using a portable cavity ring-down spectrometer, *Geochem. Geophys.*
548 *Geosystems*, 18(7), 2769–2784, doi:10.1002/2017GC006856, 2017.



- 549 Martini, F., Tassi, F., Vaselli, O., Del Potro, R., Martinez, M., del Laat, R. V. and Fernandez, E.: Geophysical,
550 geochemical and geodetical signals of reawakening at Turrialba volcano (Costa Rica) after almost 150 years of
551 quiescence, *J. Volcanol. Geotherm. Res.*, 198(3–4), 416–432, doi:10.1016/j.jvolgeores.2010.09.021, 2010.
- 552 Mason, E., Edmonds, M. and Turchyn, A. V.: Remobilization of crustal carbon may dominate volcanic arc emissions,
553 *Science*, 357(6348), 290–294, 2017.
- 554 McGee, K. A. and Gerlach, T. M.: Annual cycle of magmatic CO₂ in a tree-kill soil at Mammoth Mountain, California:
555 Implications for soil acidification, *Geology*, 26(5), 463–466, 1998.
- 556 Melián, G. V., Galindo, I., Pérez, N. M., Hernández, P. A., Fernández, M., Ramírez, C., Mora, R. and Alvarado, G.
557 E.: Diffuse Emission of Hydrogen from Poás Volcano, Costa Rica, America Central, *Pure Appl. Geophys.*, 164(12),
558 2465–2487, doi:10.1007/s00024-007-0282-8, 2007.
- 559 de Moor, J. M., Aiuppa, A., Avaró, G., Wehrmann, H., Dunbar, N., Muller, C., Tamburello, G., Giudice, G., Liuzzo,
560 M., Moretti, R., Conde, V. and Galle, B.: Turmoil at Turrialba Volcano (Costa Rica): Degassing and eruptive processes
561 inferred from high-frequency gas monitoring, *J. Geophys. Res. Solid Earth*, 121(8), 2016JB013150,
562 doi:10.1002/2016JB013150, 2016.
- 563 Newhall, C. G., Costa, F., Ratdomopurbo, A., Venezky, D. Y., Widiwijayanti, C., Win, N. T. Z., Tan, K. and Fajiculay,
564 E.: WOVODat – An online, growing library of worldwide volcanic unrest, *J. Volcanol. Geotherm. Res.*, 345, 184–
565 199, doi:10.1016/j.jvolgeores.2017.08.003, 2017.
- 566 Norby, R. J., Warren, J. M., Iversen, C. M., Medlyn, B. E. and McMurtrie, R. E.: CO₂ enhancement of forest
567 productivity constrained by limited nitrogen availability, *Proc. Natl. Acad. Sci.*, 107(45), 19368–19373,
568 doi:10.1073/pnas.1006463107, 2010.
- 569 Norby, R. J., De Kauwe, M. G., Domingues, T. F., Duursma, R. A., Ellsworth, D. S., Goll, D. S., Lapola, D. M., Luus,
570 K. A., MacKenzie, A. R., Medlyn, B. E., Pavlick, R., Rammig, A., Smith, B., Thomas, R., Thonicke, K., Walker, A.
571 P., Yang, X. and Zaehle, S.: Model–data synthesis for the next generation of forest free-air CO₂ enrichment (FACE)
572 experiments, *New Phytol.*, 209(1), 17–28, doi:10.1111/nph.13593, 2016.
- 573 Norman, E. M.: *Buddlejaceae (Flora Neotropica Monograph No. 81)*, The New York Botanical Garden Press., 2000.
- 574 Oda, T. and Maksyutov, S.: A very high-resolution (1 km×1 km) global fossil fuel CO₂ emission inventory derived
575 using a point source database and satellite observations of nighttime lights, *Atmos Chem Phys*, 11(2), 543–556,
576 doi:10.5194/acp-11-543-2011, 2011.
- 577 Paoletti, E., Seufert, G., Della Rocca, G. and Thomsen, H.: Photosynthetic responses to elevated CO₂ and O₃ in
578 *Quercus ilex* leaves at a natural CO₂ spring, *Environ. Pollut.*, 147(3), 516–524, doi:10.1016/j.envpol.2006.08.039,
579 2007.
- 580 Parry, C., Blonquist, J. M. and Bugbee, B.: In situ measurement of leaf chlorophyll concentration: analysis of the
581 optical/absolute relationship, *Plant Cell Environ.*, 37(11), 2508–2520, doi:10.1111/pce.12324, 2014.
- 582 Pérez, N., Hernandez, P., Padilla, G., Nolasco, D., Barrancos, J., Melián, G., Padrón, E., Dionis, S., Calvo, D. and
583 Rodríguez, F.: Global CO₂ emission from volcanic lakes., 2011.
- 584 Peters, W., Jacobson, A. R., Sweeney, C., Andrews, A. E., Conway, T. J., Masarie, K., Miller, J. B., Bruhwiler, L. M.
585 P., Pétron, G., Hirsch, A. I., Worthy, D. E. J., Werf, G. R. van der, Randerson, J. T., Wennberg, P. O., Krol, M. C. and



- 586 Tans, P. P.: An atmospheric perspective on North American carbon dioxide exchange: CarbonTracker, Proc. Natl.
587 Acad. Sci., 104(48), 18925–18930, doi:10.1073/pnas.0708986104, 2007.
- 588 Pieri, D., Schwandner, F. M., Realmuto, V. J., Lundgren, P. R., Hook, S., Anderson, K., Buongiorno, M. F., Diaz, J.
589 A., Gillespie, A., Miklius, A., Mothes, P., Mouginiis-Mark, P., Pallister, M., Poland, M., Palgar, L. L., Pata, F.,
590 Pritchard, M., Self, S., Sigmundsson, F., de Silva, S. and Webley, P.: Enabling a global perspective for deterministic
591 modeling of volcanic unrest, [online] Available from:
592 https://hyspiri.jpl.nasa.gov/downloads/RFI2_HyspIRI_related_160517/RFI2_final_PieriDavidC-final-rev.pdf
593 (Accessed 20 February 2018), 2016.
- 594 Pinkard, E. A., Beadle, C. L., Mendham, D. S., Carter, J. and Glen, M.: Determining photosynthetic responses of
595 forest species to elevated CO₂: alternatives to FACE, For. Ecol. Manag., 260(8), 1251–1261, 2010.
- 596 Pyle, D. M.: What Can We Learn from Records of Past Eruptions to Better Prepare for the Future?, in SpringerLink,
597 pp. 1–18, Springer, Berlin, Heidelberg., 2017.
- 598 Quintana-Ascencio, P. F., Ramírez-Marcial, N., González-Espinosa, M. and Martínez-Icó, M.: Sapling survival and
599 growth of coniferous and broad-leaved trees in successional highland habitats in Mexico, Appl. Veg. Sci., 7(1), 81–
600 88, 2004.
- 601 Rizzo, A. L., Di Piazza, A., de Moor, J. M., Alvarado, G. E., Avaró, G., Carapezza, M. L. and Mora, M. M.: Eruptive
602 activity at Turrialba volcano (Costa Rica): Inferences from ³He/⁴He in fumarole gases and chemistry of the products
603 ejected during 2014 and 2015: ERUPTIVE ACTIVITY AT TURRIALBA VOLCANO, Geochem. Geophys.
604 Geosystems, 17(11), 4478–4494, doi:10.1002/2016GC006525, 2016.
- 605 Saha, S., Moorthi, S., Pan, H.-L., Wu, X., Wang, J., Nadiga, S., Tripp, P., Kistler, R., Woollen, J., Behringer, D., Liu,
606 H., Stokes, D., Grumbine, R., Gayno, G., Wang, J., Hou, Y.-T., Chuang, H., Juang, H.-M. H., Sela, J., Iredell, M.,
607 Treadon, R., Kleist, D., Van Delst, P., Keyser, D., Derber, J., Ek, M., Meng, J., Wei, H., Yang, R., Lord, S., van den
608 Dool, H., Kumar, A., Wang, W., Long, C., Chelliah, M., Xue, Y., Huang, B., Schemm, J.-K., Ebisuzaki, W., Lin, R.,
609 Xie, P., Chen, M., Zhou, S., Higgins, W., Zou, C.-Z., Liu, Q., Chen, Y., Han, Y., Cucurull, L., Reynolds, R. W.,
610 Rutledge, G. and Goldberg, M.: NCEP Climate Forecast System Reanalysis (CFSR) 6-hourly Products, January 1979
611 to December 2010, Bull. Am. Meteorol. Soc., 91(8), 1015–1058, doi:10.5065/D69K487J, 2010a.
- 612 Saha, S., Moorthi, S., Pan, H.-L., Wu, X., Wang, J., Nadiga, S., Tripp, P., Kistler, R., Woollen, J., Behringer, D., Liu,
613 H., Stokes, D., Grumbine, R., Gayno, G., Wang, J., Hou, Y.-T., Chuang, H., Juang, H.-M. H., Sela, J., Iredell, M.,
614 Treadon, R., Kleist, D., Van Delst, P., Keyser, D., Derber, J., Ek, M., Meng, J., Wei, H., Yang, R., Lord, S., van den
615 Dool, H., Kumar, A., Wang, W., Long, C., Chelliah, M., Xue, Y., Huang, B., Schemm, J.-K., Ebisuzaki, W., Lin, R.,
616 Xie, P., Chen, M., Zhou, S., Higgins, W., Zou, C.-Z., Liu, Q., Chen, Y., Han, Y., Cucurull, L., Reynolds, R. W.,
617 Rutledge, G. and Goldberg, M.: The NCEP Climate Forecast System Reanalysis, Bull. Am. Meteorol. Soc., 91(8),
618 1015–1058, doi:10.1175/2010BAMS3001.1, 2010b.
- 619 Saurer, M., Cherubini, P., Bonani, G. and Siegwolf, R.: Tracing carbon uptake from a natural CO₂ spring into tree
620 rings: an isotope approach, Tree Physiol., 23(14), 997–1004, doi:10.1093/treephys/23.14.997, 2003.
- 621 Schimel, D., Stephens, B. B. and Fisher, J. B.: Effect of increasing CO₂ on the terrestrial carbon cycle, Proc. Natl.
622 Acad. Sci., 112(2), 436–441, doi:10.1073/pnas.1407302112, 2015.



- 623 Schwandner, F. M., Seward, T. M., Gize, A. P., Hall, P. A. and Dietrich, V. J.: Diffuse emission of organic trace gases
624 from the flank and crater of a quiescent active volcano (Vulcano, Aeolian Islands, Italy), *J. Geophys. Res.*
625 *Atmospheres*, 109(D4), D04301, doi:10.1029/2003JD003890, 2004.
- 626 Schwandner, F. M., Gunson, M. R., Miller, C. E., Carn, S. A., Eldering, A., Krings, T., Verhulst, K. R., Schimel, D.
627 S., Nguyen, H. M., Crisp, D., O'Dell, C. W., Osterman, G. B., Iraci, L. T. and Podolske, J. R.: Spaceborne detection
628 of localized carbon dioxide sources, *Science*, 358(6360), eaam5782, doi:10.1126/science.aam5782, 2017.
- 629 Sharma, S. and Williams, D.: Carbon and oxygen isotope analysis of leaf biomass reveals contrasting photosynthetic
630 responses to elevated CO₂ near geologic vents in Yellowstone National Park, *Biogeosciences*, 6(1), 25,
631 doi:10.5194/bg-6-25-2009, 2009.
- 632 Shinohara, H., Aiuppa, A., Giudice, G., Gurrieri, S. and Liuzzo, M.: Variation of H₂O/CO₂ and CO₂/SO₂ ratios of
633 volcanic gases discharged by continuous degassing of Mount Etna volcano, Italy, *J. Geophys. Res. Solid Earth*,
634 113(B9), doi:10.1029/2007JB005185, 2008.
- 635 Sinclair, A. J.: Selection of threshold values in geochemical data using probability graphs, *J. Geochem. Explor.*, 3(2),
636 129–149, doi:10.1016/0375-6742(74)90030-2, 1974.
- 637 Sorey, M. L., Evans, W. C., Kennedy, B. M., Farrar, C. D., Hainsworth, L. J. and Hausback, B.: Carbon dioxide and
638 helium emissions from a reservoir of magmatic gas beneath Mammoth Mountain, California, *J. Geophys. Res. Solid*
639 *Earth*, 103(B7), 15303–15323, doi:10.1029/98JB01389, 1998.
- 640 Sparks, R. S. J., Biggs, J. and Neuberg, J. W.: Monitoring Volcanoes, *Science*, 335(6074), 1310–1311,
641 doi:10.1126/science.1219485, 2012.
- 642 Staebler, R. M. and Fitzjarrald, D. R.: Observing subcanopy CO₂ advection, *Agric. For. Meteorol.*, 122(3–4), 139–
643 156, doi:10.1016/j.agrformet.2003.09.011, 2004.
- 644 Stine, C. M. and Banks, N. G.: Costa Rica Volcano Profile, USGS Numbered Series, U.S. Geological Survey. [online]
645 Available from: <https://pubs.er.usgs.gov/publication/ofr91591>, 1991.
- 646 Stohl, A. and Thomson, D. J.: A Density Correction for Lagrangian Particle Dispersion Models, *Bound.-Layer*
647 *Meteorol.*, 90(1), 155–167, doi:10.1023/A:1001741110696, 1999.
- 648 Stohl, A., Hittenberger, M. and Wotawa, G.: Validation of the Lagrangian particle dispersion model FLEXPART
649 against large-scale tracer experiment data, *Atmos. Environ.*, 32(24), 4245–4264, 1998.
- 650 Stohl, A., Forster, C., Frank, A., Seibert, P. and Wotawa, G.: Technical note: The Lagrangian particle dispersion model
651 FLEXPART version 6.2, *Atmospheric Chem. Phys.*, 5(9), 2461–2474, doi:<https://doi.org/10.5194/acp-5-2461-2005>,
652 2005.
- 653 Symonds, R. B., Gerlach, T. M. and Reed, M. H.: Magmatic gas scrubbing: implications for volcano monitoring, *J.*
654 *Volcanol. Geotherm. Res.*, 108(1), 303–341, doi:10.1016/S0377-0273(00)00292-4, 2001.
- 655 Tanner, E. V. J., Vitousek, P. M. and Cuevas, E.: Experimental Investigation of Nutrient Limitation of Forest Growth
656 on Wet Tropical Mountains, *Ecology*, 79(1), 10–22, doi:10.1890/0012-9658(1998)079[0010:EIONLO]2.0.CO;2,
657 1998.
- 658 Tercek, M. T., Al-Niemi, T. S. and Stout, R. G.: Plants Exposed to High Levels of Carbon Dioxide in Yellowstone
659 National Park: A Glimpse into the Future?, *Yellowstone Sci.*, 16(1), 12–19, 2008.



- 660 Thomas, C. K.: Variability of Sub-Canopy Flow, Temperature, and Horizontal Advection in Moderately Complex
661 Terrain, *Bound.-Layer Meteorol.*, 139(1), 61–81, doi:10.1007/s10546-010-9578-9, 2011.
- 662 Townsend, A. R., Cleveland, C. C., Houlton, B. Z., Alden, C. B. and White, J. W.: Multi-element regulation of the
663 tropical forest carbon cycle, *Front. Ecol. Environ.*, 9(1), 9–17, doi:10.1890/100047, 2011.
- 664 Viveiros, F., Ferreira, T., Silva, C. and Gaspar, J.: Meteorological factors controlling soil gases and indoor CO₂
665 concentration: A permanent risk in degassing areas, *Sci. Total Environ.*, 407(4), 1362–1372,
666 doi:10.1016/j.scitotenv.2008.10.009, 2009.
- 667 Weng, C., Bush, M. B. and Chepstow-Lusty, A. J.: Holocene changes of Andean alder(*Alnus acuminata*) in highland
668 Ecuador and Peru, *J. Quat. Sci.*, 19(7), 685–691, doi:10.1002/jqs.882, 2004.
- 669 Werner, C., Kelly, P. J., Doukas, M., Lopez, T., Pfeffer, M., McGimsey, R. and Neal, C.: Degassing of CO₂, SO₂, and
670 H₂S associated with the 2009 eruption of Redoubt Volcano, Alaska, *J. Volcanol. Geotherm. Res.*, 259, 270–284,
671 doi:10.1016/j.jvolgeores.2012.04.012, 2013.
- 672 Werner, C., Bergfeld, D., Farrar, C. D., Doukas, M. P., Kelly, P. J. and Kern, C.: Decadal-scale variability of diffuse
673 CO₂ emissions and seismicity revealed from long-term monitoring (1995–2013) at Mammoth Mountain, California,
674 USA, *J. Volcanol. Geotherm. Res.*, 289, 51–63, doi:10.1016/j.jvolgeores.2014.10.020, 2014.
- 675 Williams-Jones, G.: The Distribution and Origin of Radon, CO₂ and SO₂ Gases at Arenal Volcano, Costa Rica,
676 Université de Montréal., 1997.
- 677 Williams-Jones, G., Stix, J., Heiligmann, M., Charland, A., Lollar, B. S., Arner, N., Garzón, G. V., Barquero, J. and
678 Fernandez, E.: A model of diffuse degassing at three subduction-related volcanoes, *Bull. Volcanol.*, 62(2), 130–142,
679 2000.
- 680
- 681



682
683

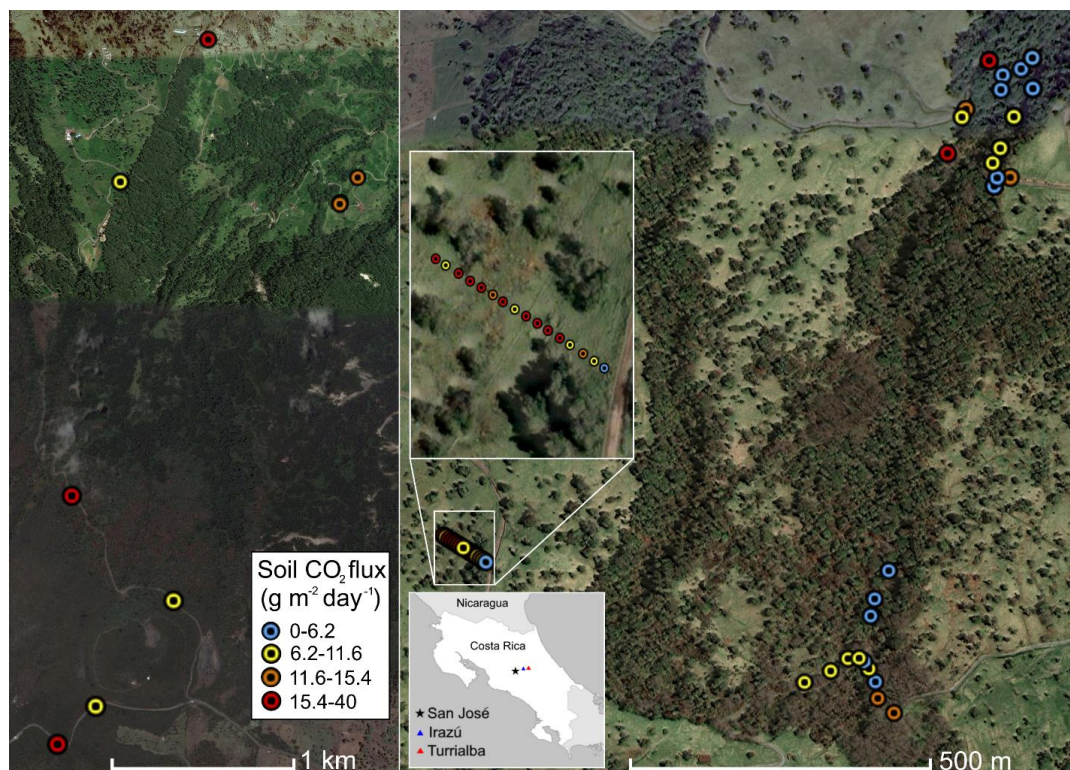


Fig. 1: Overview of measurement locations in two old-growth forests on the upper flanks of two active volcanoes in Costa Rica, Turrialba and Irazú. Distribution of mean soil CO₂ flux across north flank of Irazú (left) and south flank of Turrialba (right). Colors of dots correspond to flux populations (see Fig. 3).



684

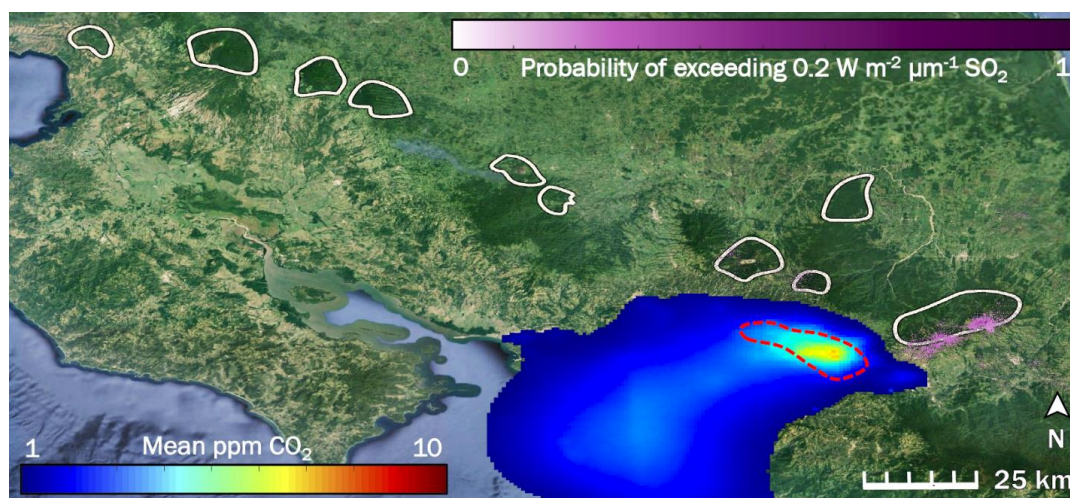


Fig. 2: The influence of two potentially confounding gases on our study area (right hand white polygon) in Costa Rica is low to non-existent: anthropogenic CO₂ from San José (blue to red color scale), and volcanic SO₂ (purple color scale). White polygons are drawn around locations of the forested active volcanic edifices in Costa Rica. The dashed red line indicates the rough border of the San José urban area. Prevailing winds throughout the year consistently blow all anthropogenic CO₂ away from our study area and from all other white polygons.



685
686
687

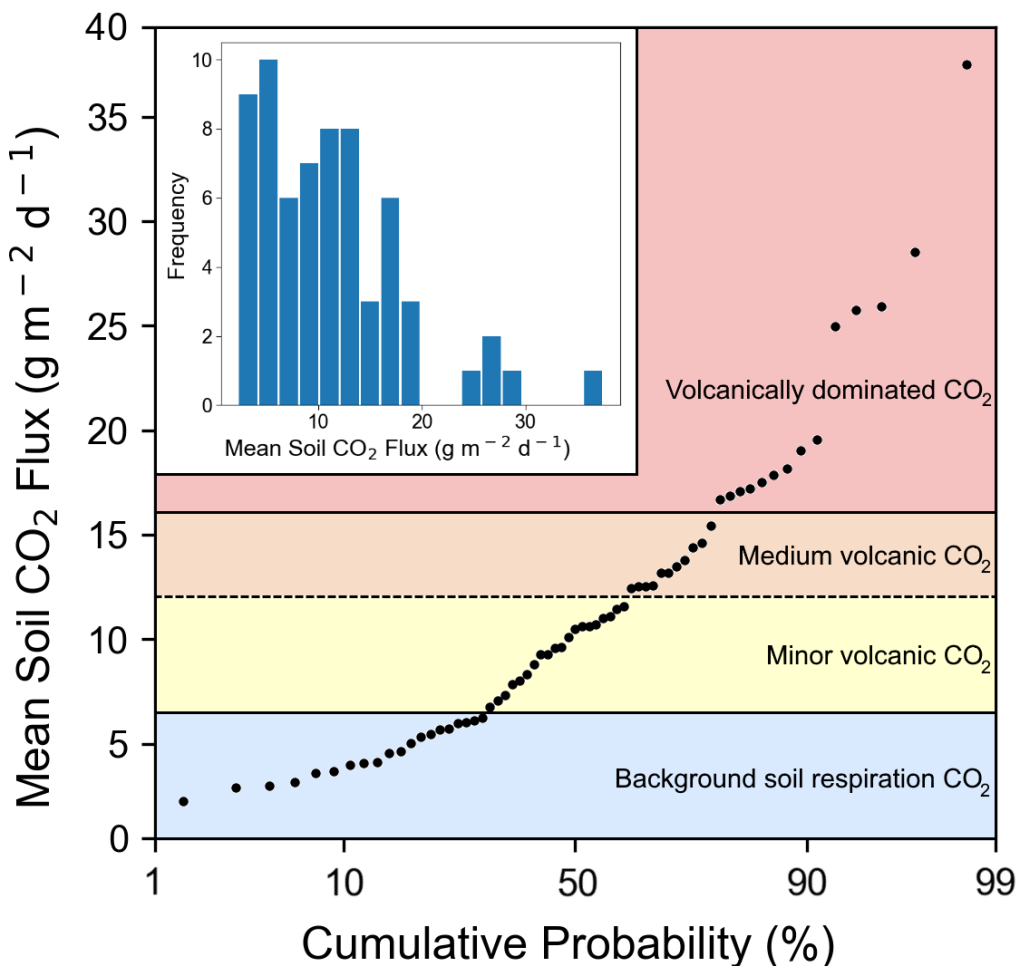


Fig 3: Soil CO₂ flux into the sub-canopy air of forests on the Turrialba-Irazú volcanic complex is pervasively and significantly influenced by a deep volcanic gas source. At least four different overlapping populations of soil CO₂ flux were identified, using a cumulative probability plot, where inflection points indicate population boundaries (Sinclair 1974). 69% of sampling locations (45 total) are exposed to varying degrees of volcanically derived elevated CO₂. Populations are color-coded based on the same color scale as Fig. 1.



688

689

690

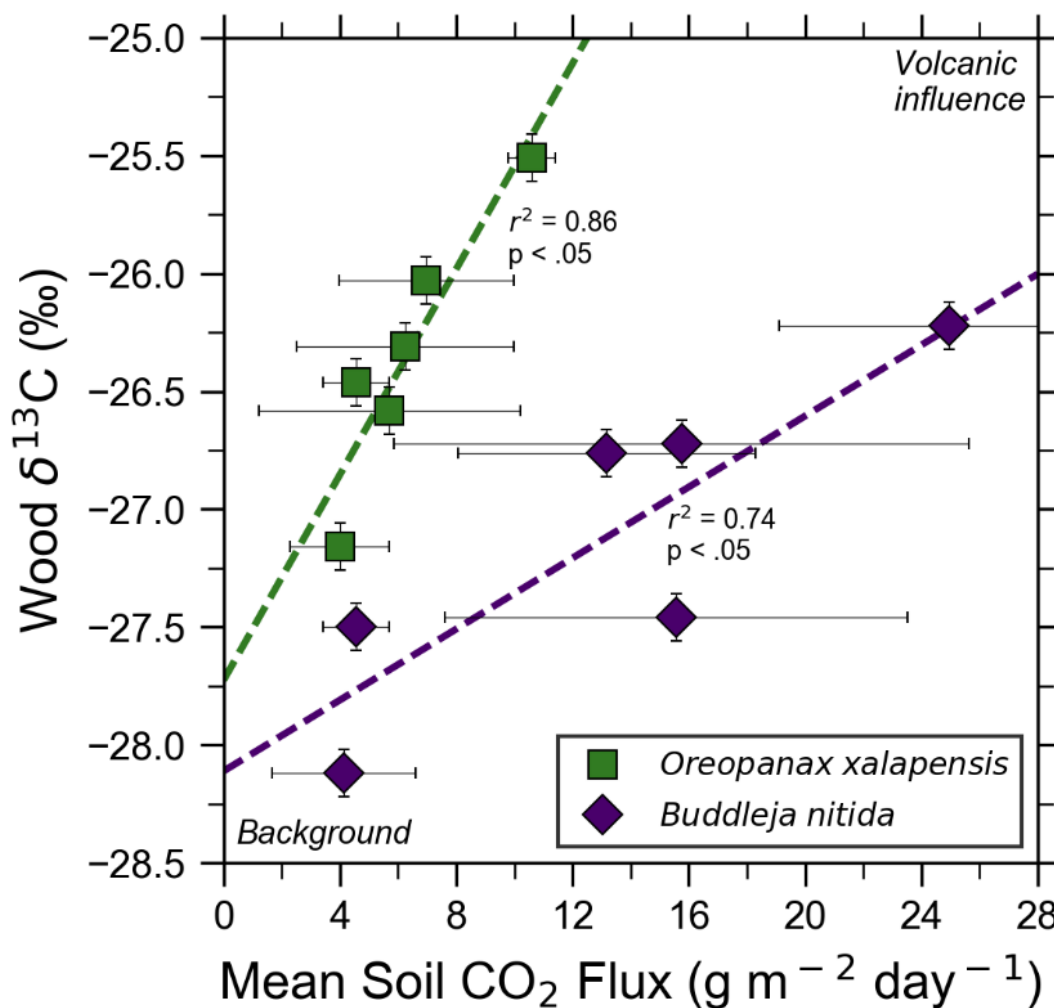


Fig 4: Bulk wood $\delta^{13}\text{C}$ of trees on Costa Rica's Turrialba volcano shows strong correlations with increasing volcanic CO_2 flux for two species, *O. xalapensis* and *B. nitida*, indicating long-term photosynthetic incorporation of isotopically heavy volcanic CO_2 . Stable carbon isotope ratio ($\delta^{13}\text{C}$) of wood cores are plotted against soil CO_2 flux measured immediately adjacent to the tree that the core sample was taken from. Background and volcanic influence labels apply to both axes – higher CO_2 flux and heavier (less negative) $\delta^{13}\text{C}$ values are both characteristic of volcanic CO_2 emissions.



691

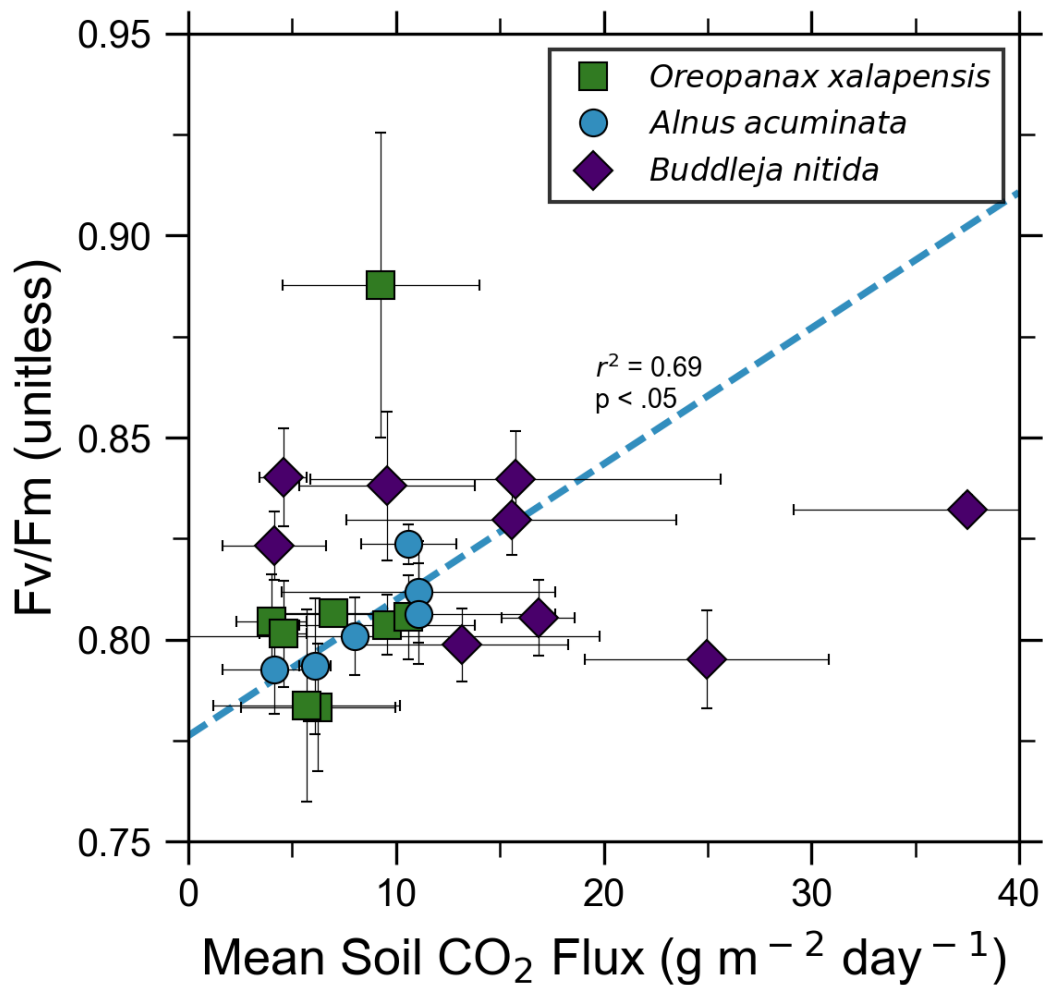
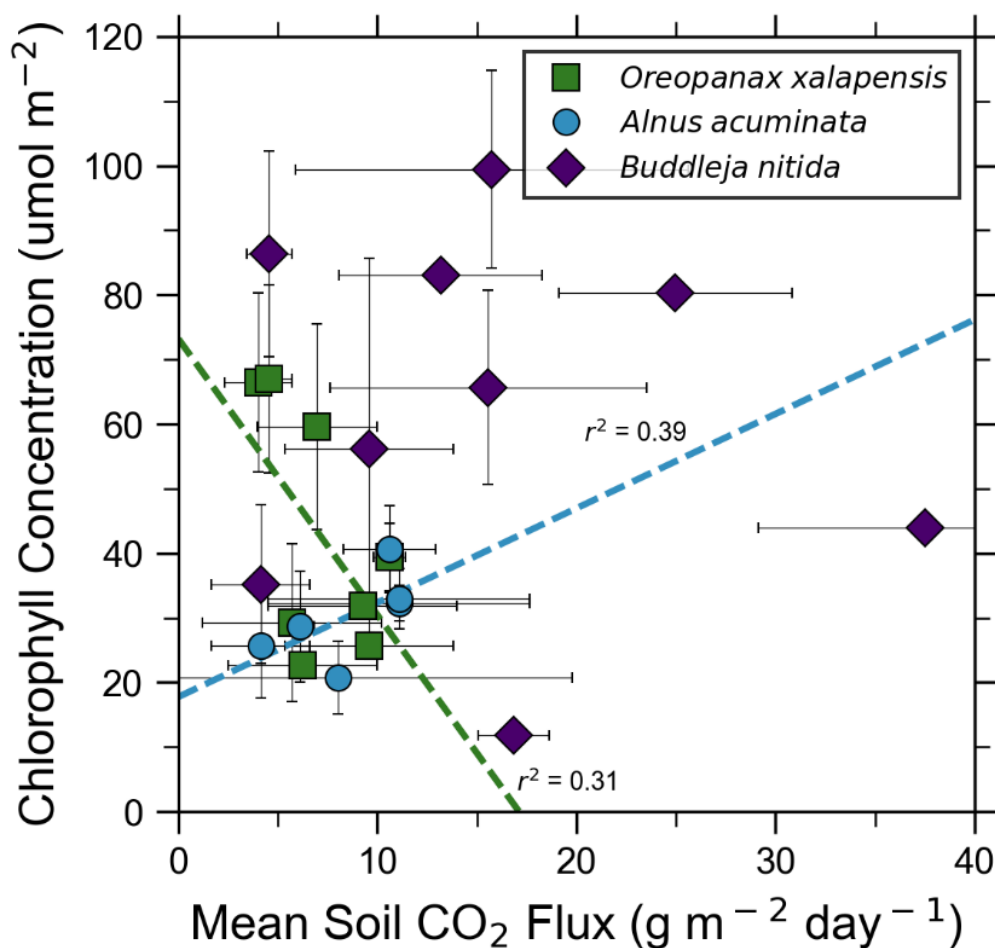


Fig. 5: Photosynthetic activity of some tree species in old-growth forests on the upper flanks of two active volcanoes in Costa Rica, Turrialba and Irazú, may show short-term response to volcanically elevated CO₂. Leaf fluorescence (Fv/Fm) and soil CO₂ flux were strongly correlated for *A. acuminata*, but not for other species.

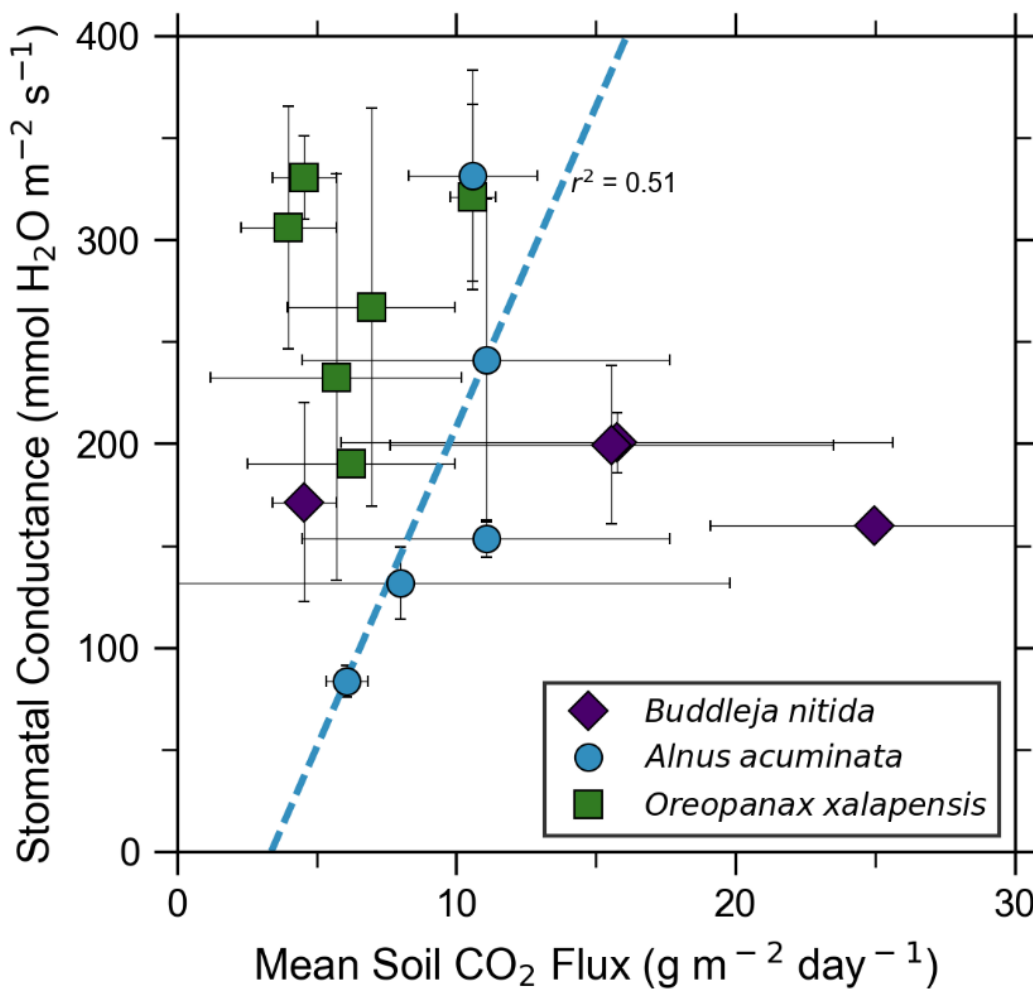


692

Fig. 6: Some tree species in old-growth forests on the upper flanks of two active volcanoes in Costa Rica, Turrialba and Irazú, may express their short-term response to volcanically elevated CO₂ by producing more chlorophyll. A species that showed strong short-term response (*A. Acuminata*, Fig. 5) also shows a positive correlation between chlorophyll concentration and mean soil CO₂ flux.

693

694



695

Fig. 7: Leaf stomatal conductance of a tree species that strongly responds to volcanically elevated CO₂ (Figs. 5, 6) has positive correlations with volcanic CO₂ flux, consistent with increased gas-exchange.

696